



Transoceanic wave propagation links iceberg calving margins of Antarctica with storms in tropics and Northern Hemisphere

Douglas R. MacAyeal,¹ Emile A. Okal,² Richard C. Aster,³ Jeremy N. Bassis,⁴ Kelly M. Brunt,¹ L. Mac. Cathles,¹ Robert Drucker,⁵ Helen A. Fricker,⁴ Young-Jin Kim,¹ Seelye Martin,⁵ Marianne H. Okal,¹ Olga V. Sergienko,⁸ Mark P. Sponsler,⁶ and Jonathan E. Thom⁷

Received 14 June 2006; accepted 31 July 2006; published 12 September 2006.

[1] We deployed seismometers on the Ross Ice Shelf and on various icebergs adrift in the Ross Sea (including B15A, a large 100 km by 30 km fragment of B15, which calved from the Ross Ice Shelf in March, 2000). The data reveal that the dominant energy of these floating ice masses is in the 0.01 to 0.1 Hz band, and is associated with sea swell generated in the tropical and extra-tropical Pacific Ocean. In one example, a strong storm in the Gulf of Alaska on 21 October 2005, approximately 13,500 km from the Ross Sea, generated swell that arrived at B15A immediately prior to, and during, its break-up off Cape Adare on 27 October 2005. If sea swell influences iceberg calving and break-up, a teleconnection exists between the Antarctic ice sheet mass balance and weather systems worldwide. **Citation:** MacAyeal, D. R., et al. (2006), Transoceanic wave propagation links iceberg calving margins of Antarctica with storms in tropics and Northern Hemisphere, *Geophys. Res. Lett.*, 33, L17502, doi:10.1029/2006GL027235.

1. Introduction

[2] Over the past 5 years, we have deployed various instruments on large tabular icebergs originating from the Ross Ice Shelf [Lazzara et al., 1999; Long et al., 2002] and on the ice shelf itself to study calving and the nature of iceberg drift, melting and disintegration. A curious consequence of iceberg activity in the Ross Sea has been the observation of ‘iceberg songs’ (tremor distinguished by numerous multiples of a fundamental frequency around a few Hz) as *T* phases at various seismological sites in Antarctica [Müller et al., 2005; Romero, 2004] and on islands

in the Pacific [Talandier et al., 2002]. To investigate the origin of this tremor, we placed Guralp 40T[™] seismometers with Quanterra[™] digitizing and data recording equipment (provided by PASSCAL) on the floating Ross Ice Shelf (Nascent Iceberg – an incipient calving site) and on icebergs B15A, B15K and C16 (Figure 1). An unanticipated benefit of this effort was the discovery that the seismometers we deployed recorded motions of the ocean surface in the low-frequency band (0.01 to 0.15 Hz), including sea swell and various tsunamis. In this letter, we report our analysis of sea-swell observations on the icebergs and ice shelf, and display evidence for trans-Pacific propagation of swell that reaches the Antarctic iceberg calving margin.

2. Sea Swell Dominates Energy Spectrum

[3] The seismometer on Nascent Iceberg (the Ross Ice Shelf) collected data for 170 days out of a total of 363 during its 2004–2005 deployment (all instruments shut down during the season of winter darkness, due to reliance on photovoltaic power). A spectrogram constructed from the 1-Hz time series of the seismometer vertical channel (Figure 2) shows that energy density in the 0.01 to 0.06 Hz frequency band is temporally variable on a week-to-week basis. (Close inspection also shows variability at shorter time scales associated with normal earthquake events and other phenomena not associated with ocean waves.) A window of increased amplitude from Mid December 2004 to Mid March 2005 corresponds to the period when boreal-winter storms in the North Pacific are most frequent [Whittaker and Horn, 1984], and to the typhoon season in the South Pacific. It is likely that the austral winter storms of the Southern Ocean also contribute energy to the ice shelf, however, our instruments could not verify this due to shut-down of their power supply (solar panels).

[4] A close examination of the brightest part of the spectrogram during the boreal winter (Figure 2) reveals a mosaic of organized ‘slanting swaths’ of increased spectral energy density similar to spectrogram figures shown in Munk et al. [1963] and Snodgrass et al. [1966]. These swaths begin at low frequencies and progressively increase their frequencies with time, because the group velocity, U , for surface gravity waves on deep water increases with decreasing frequency. An asymptotic expression for the group velocity valid in deep water is $U = g/(4\pi f)$, where f is frequency (in Hz) and g is the acceleration of gravity [Munk et al., 1963]. This relationship permits estimation of the distance, d , and travel time, t_o , linking a given wave origin (a storm) to the receiver (a seismometer on an iceberg

¹Department of the Geophysical Sciences, University of Chicago, Chicago, Illinois, USA.

²Department of Geological Sciences, Northwestern University, Evanston, Illinois, USA.

³Geophysical Research Center and Department of Earth and Environmental Science, New Mexico Institute of Mining and Technology, Socorro, New Mexico, USA.

⁴Institute for Geophysics and Planetary Physics, Scripps Institution of Oceanography, University of California, San Diego, La Jolla, California, USA.

⁵School of Oceanography, University of Washington, Seattle, Washington, USA.

⁶Stormsurf, Half Moon Bay, California, USA.

⁷Antarctic Meteorological Research Centre, University of Wisconsin, Madison, Wisconsin, USA.

⁸Hydrospheric and Biospheric Sciences Laboratory, NASA Goddard Space Flight Center, Greenbelt, Maryland, USA.

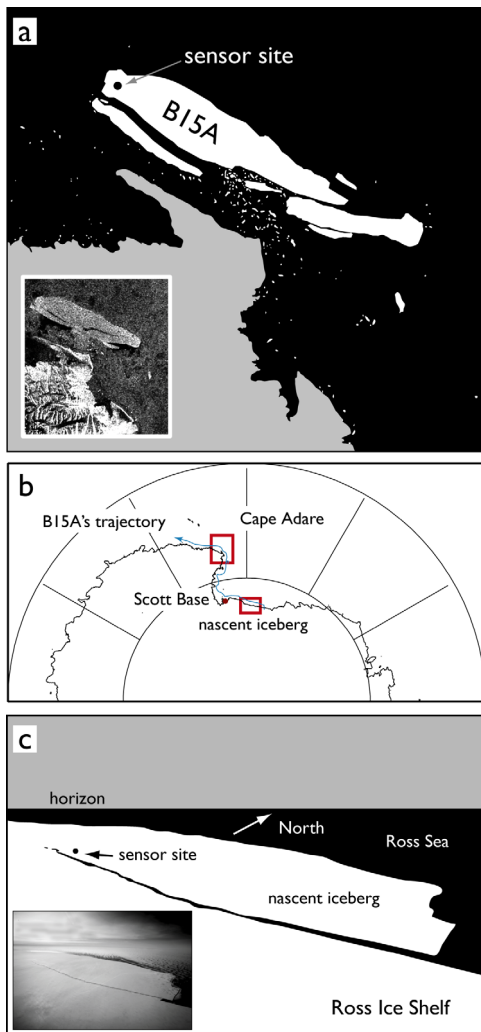


Figure 1. Seismometer locations and arrangement of field sites. (a) Sketch map of iceberg B15A following its break-up on October 27, 2005, near Cape Adare and the Possession Islands, Antarctica. Satellite radar image of B15A (inset) on 30 October, 2005, (image credit: ESA/Envisat). (b) Pacific-facing sector of Antarctica. Approximate drift trajectory of B15A shown in blue. (c) Aerial photograph of Nascent Iceberg on the Ross Ice Shelf, Antarctica. (photo credit: Joseph Harrigan, Raytheon Polar Services Co.).

or ice shelf). For each energy-density swath in the spectrogram of Figure 2, $d = g/(4\pi) (df/dt)^{-1}$, and $t_o = d/U$, where df/dt is the slope of the swath. Figure 2 highlights two examples of slanted energy-density swaths for which d and t_o are computed. In one example (labeled Gulf of Alaska), the distance to the wave source is 13,450 km. In the other example (labeled Typhoon Olaf), the distance to the wave source is 5,950 km.

3. Analysis of Meteorological Data and Wave Dispersion

[5] Focusing on the first, most-distant example (Gulf of Alaska), the time of swell origin, t_o , is 21 October 2005 – about 6 days before the first swell (with $f \sim 0.01$ Hz) arrived

in the Ross Sea. To verify this remarkable transoceanic propagation, we examined various meteorological data to identify the source of the swell in the North Pacific. Although uncertainty in the source/receiver distance and time of origin is approximately 1000 km, and 12 hours, the large spatial scale and duration of storms in the North Pacific render it easy to identify the meteorological origin of the swell. A scan of on-line meteorological records, geostationary weather satellite imagery (Figure 3a), and analysis of wave-height models performed in the context of surf forecasts (Figure 3b) confirmed a large, extra-tropical cyclone in the Gulf of Alaska on 20–21 October 2005.

[6] To additionally test the hypothesis that a Gulf of Alaska storm was the origin of swell observed in Antarctica beginning 27 October 2005, we examined seismometer and deep-sea buoy wave-height records for stations along a North-South transect of the Pacific (Figure 3c). Our goal was to see if the sea-swell energy in question could be detected in transit at other locations along a line between the storm (approximately 47° N, 155° W) and Antarctica. On Pitcairn Island (25.07° S; 130.10° W; at 5 km^2 the smallest seismically instrumented island in the Pacific basin) this sea swell and associated microseism [Longuet-Higgins, 1950] were recorded approximately 2 days prior to the arrival of

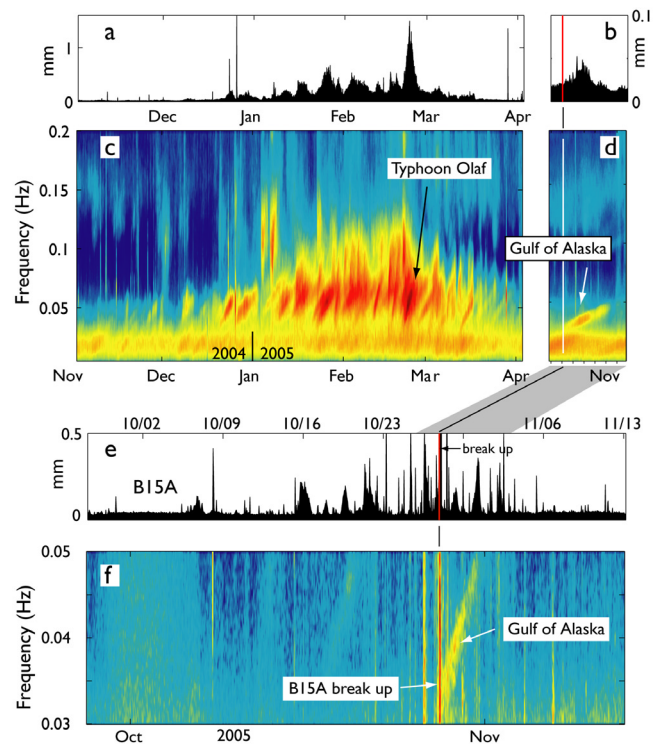


Figure 2. Seismometer data. Nascent Iceberg 1-Hz vertical channel amplitude envelope, (a) November 2004 to April 2005 and (b) 25 October to 2 November, 2005. The vertical line denotes the approximate time of B15A break-up (21:00 on 27 October 2005). Spectrogram of Nascent Iceberg data ((c) November 2004 to April 2005, (d) 25 October to 2 November, 2005). White spaces between panels represent time when seismometer data was not recorded (no power). (e) The B15A 1-Hz vertical channel amplitude envelope and (f) spectrogram for 27 September to 14 November, 2005.

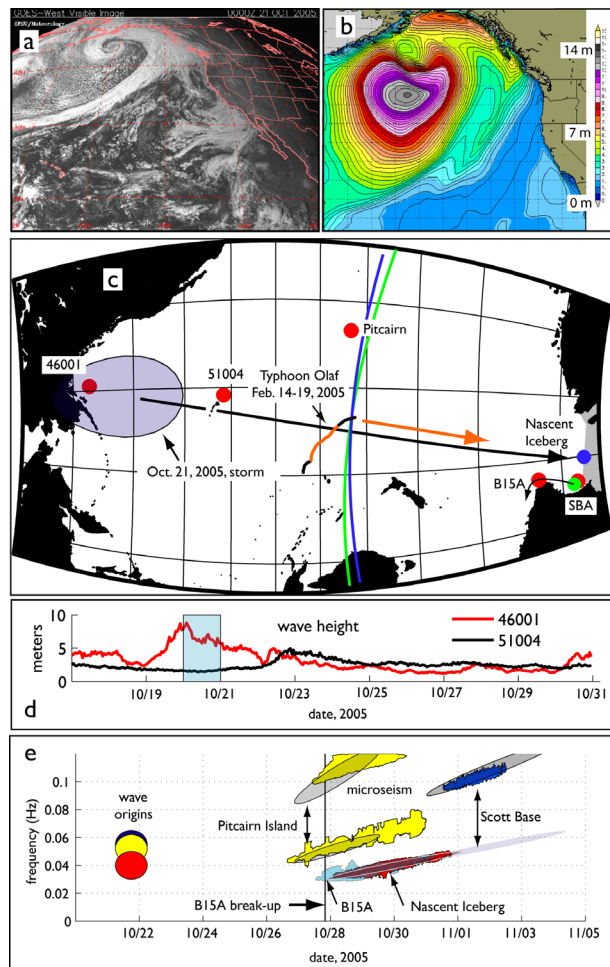


Figure 3. Analysis of swell in transit from Gulf of Alaska to Antarctica, and track of Typhoon Olaf. (a) GOES West image of storm on 21 October 2005 at 0000 UTC. (b) Model wave-height estimate for 21 October 2005 at 1200 UTC (c.i. 0.6 m). (c) Location map and track of Typhoon Olaf during 14–19 February 2005, when it was category 3 or greater. B15A's location at time of break-up is shown as a red dot. Period where the typhoon was category 5 indicated in orange color. Circles intersecting on the track near the typhoon's position on 19 February 2005 represent the triangulated position implied by B15A (green dot near SBA, reflecting its position at the time) and Nascent Iceberg (blue) data. (d) Wave-height records of NOAA buoys 46001 and 51004. Blue bar represents time of lowest barometer reading at NOAA buoy 46001. (e) Idealized and observed energy-density maxima on frequency vs. time plot. Red, yellow and blue circles on 21 October 2005 represent energy-density maxima at source, and grey ellipses represent energy-density maxima after deformation by dispersion. Predicted and observed microseism (for Pitcairn and Scott Base, labeled SBA in Figure 3c) appear at frequencies above 0.08 Hz. Colour patches represent observations abstracted from spectrograms at Pitcairn Island and various Antarctic sites (yellow = Pitcairn Island, light blue = B15A, red = Nascent Iceberg, dark blue = Scott Base) and are where the energy density associated with these observations exceeded 85% of the local mean. The patches have been trimmed (arbitrarily, removing vertical extents) to eliminate signal not associated with swell (e.g., earthquakes).

the swell in Antarctica (Figure 3e), which is consistent with the propagation characteristics of a single group of waves traversing the Pacific. Wave-heights recorded by deep-sea buoys in the Gulf of Alaska and Hawaii (NOAA buoys 46001 and 51001, respectively) reveal the amplitude of the waves at the origin of the storm (~ 10 m amplitude) and near the Hawaiian Islands (~ 5 m amplitude) about 3 days after starting their southbound travel (Figure 3d).

[7] For the second, most energetic example of swell recorded on the icebergs and ice shelf (labeled Typhoon Olaf in Figure 2a, and occurring between 21 and 26 February 2005), the above methodology revealed a tropical origin: a category 5 hurricane that passed near the Cook Islands over the period 14–19 February 2005 (Figure 3c). Owing to the relative proximity to the Ross Sea of the typhoon's track, and to the separation of B15A and Nascent Iceberg receiving sites on a line perpendicular to the direction of wave propagation, the source of wave origin could be determined by triangulation using the two values of d computed from the spectrograms. The result (Figure 3c) confirms a location near the southern end of the typhoon's track.

4. Sea Swell: An Agent in Iceberg Calving and Break-Up?

[8] Considering the long history of investigation into trans-oceanic propagation of long-period ocean waves [Munk *et al.*, 1963; Snodgrass *et al.*, 1966], it is not surprising that our observations have revealed examples of sea swell traveling half-way around the earth to shake icebergs and ice shelves along a broad swath of the Antarctic coastline. What is unique about the observations presented here is that they imply that giant icebergs and the calving margins of major ice shelves are mechanically influenced by meteorological conditions in the far field. Considering that iceberg calving is involved in the maintenance of Antarctica's ice-mass budget [Jacobs *et al.*, 1992], it is thus natural to consider whether climate conditions in the extra-tropical northern hemisphere and the tropics (e.g., storm intensity or hurricane/typhoon frequency) could exert a control on the mass budget of the Antarctic Ice Sheet.

[9] A leading hypothesis for how tabular icebergs are calved concerns swell-induced vibration that can fatigue and fracture ice at weak spots, producing rifts that become iceberg-detachment boundaries [Holdsworth and Glynn, 1978; Kristensen *et al.*, 1982; Zwally *et al.*, 2002]. With this hypothesis in mind, we considered whether the arrival of swell from the Gulf of Alaska storm discussed above contributed to the spectacular break-up of B15A on October 27 2005 (Figure 1a).

[10] The drift trajectory of the iceberg observed by on-board GPS and satellite images showed that immediately prior to break-up the iceberg grounded on the shoals adjacent to the Possession Islands near Cape Adare. For 27 and 28 October 2005, comparison of geo-referenced MODIS imagery and the F. Davey and S. S. Jacobs (personal communication, 2005) bottom topography shows that the midpoint of B-15A grounded on the shoals and suffered longitudinal fractures at the point of grounding. The time of this break-up was about 2100 UTC on 27 October – about 12 hours after swell from the Gulf of Alaska storm was observed in the seismic record. This time of break-up and its

association with grounding is suggested additionally by the fact that iceberg-generated tremor was observed in the far field – at Scott Base (labeled SBA in Figure 3c) and South Pole. The timing of arrivals at Scott Base and South Pole are consistent with solid-earth propagation of the tremor (as a *P*-wave in the crust), and this additionally supports contact of the iceberg with the seabed at the time of break-up. Also, from QuikSCAT iceberg imagery provided by D. Long (personal communication, 2006), B15B broke up at approximately the same location (B15B is another piece of the original B15, and thus has a draft similar to B15A). These two cases imply that the shoal adjacent to the Possession Islands may be habitually involved in iceberg break-up as icebergs exit the Ross Sea. Finally, the sea swell amplitude associated with the Gulf of Alaska storm was rather small (~ 1 mm) at the location of the B15A seismometer (Figure 1a), and it is difficult to account for such dramatic results from such diminutive forcing, even considering wave amplification in the area of shoaling.

[11] While a connection between sea swell and break-up of B15A remains unproven, the possible role of sea swell as a long-term effect promoting iceberg calving should not be dismissed. Of all the signals at frequencies higher than 0.01 Hz observed at Nascent, the strongest were associated with swell generated by distant storms. It may be that long-term (decadal) exposure of rifted ice-shelf calving margins to the effects of swell may contribute to fatigue and fracture of the ice-shelf detachment rifts necessary to form icebergs. This idea remains open to further investigation [e.g., *Bassis et al.*, 2005].

5. Concluding Remarks

[12] The influence of ocean swell from distant storms on the Antarctic calving margin has implications for the study of abrupt climate change in the Northern Hemisphere [*Hemming*, 2004; *Hulbe et al.*, 2004; *Knutti et al.*, 2004]. The sudden release of icebergs into the glacial North Atlantic, i.e., Heinrich events, is associated with many of the abrupt, millennial-scale shifts in glacial climate observed in the Greenland ice-core record. The mechanism that determines calving rates apparently acts on geographically separated calving fronts, causing icebergs to be released simultaneously (in an annual or decadal time-frame), as is evident from provenance studies of ice-rafted debris (IRD) blanketing the North Atlantic floor [*Grousset et al.*, 1993]. Here we demonstrate that one such mechanism could involve the effects of storm-generated sea swell. An increase in North Atlantic storminess during times of extreme cold and thermohaline circulation shutdown could create an environment of stronger and more frequent wave/ice interaction along the iceberg calving margins surrounding the North Atlantic (e.g., in a manner similar to recent increase of wave activity in the North Atlantic suggested by *Carter and Draper* [1988]). This suggestion further highlights the role of sea swell as an environmental process capable of influencing climate [*Melville*, 1996].

[13] **Acknowledgments.** Financial and logistical support was generously provided by the National Science Foundation (NSF) under the following grants: OPP-0229546; OPP-0229492, OPP-0230028, and OPP-0229305. S.M. and R.D. gratefully acknowledge the support of NASA under contract NNG04GM69G. Instruments were provided by the PASS-

CAL facility of the Incorporated Research Institutions for Seismology (IRIS) through the PASSCAL Instrument Center at New Mexico Tech. IRIS facilities are supported by Cooperative Agreement NSF EAR-000430 and the Department of Energy National Nuclear Security Administration.

References

- Bassis, J. N., R. Coleman, H. A. Fricker, and J. B. Minster (2005), Episodic propagation of a rift on the Amery Ice Shelf, East Antarctica, *Geophys. Res. Lett.*, *32*, L06502, doi:10.1029/2004GL022048.
- Carter, D. J. T., and L. Draper (1988), Has the northeast Atlantic become rougher?, *Nature*, *332*, 494.
- Grousset, F. E., L. Labeyrie, J. A. Sinko, M. Cremer, G. Bond, J. Duprat, E. Cortijo, and S. Huon (1993), Patterns of ice-rafted detritus in the glacial north Atlantic (40–55°N), *Paleoceanography*, *8*, 175–192.
- Hemming, S. R. (2004), Heinrich events: Massive late Pleistocene detritus layers of the North Atlantic and their global climate imprint, *Rev. Geophys.*, *42*, RG1005, doi:10.1029/2003RG000128.
- Holdsworth, G., and J. Glynn (1978), Iceberg calving from floating glaciers by a vibrating mechanism, *Nature*, *274*, 464–466.
- Hulbe, C. L., D. R. MacAyeal, G. H. Denton, J. Kleman, and T. V. Lowell (2004), Catastrophic ice-shelf break-up as the source of Heinrich-event icebergs, *Paleoceanography*, *19*, PA1004, doi:10.1029/2003PA000890.
- Jacobs, S. S., H. Helmer, C. S. M. Doake, A. Jenkins, and R. M. Frolich (1992), Melting of the ice shelves and the mass balance of Antarctica, *J. Glaciol.*, *38*, 375–387.
- Knutti, R., J. Flückiger, T. F. Stocker, and A. Timmermann (2004), Strong hemispheric coupling of glacial climate through freshwater discharge and ocean circulation, *Nature*, *430*, 851–856.
- Kristensen, M., V. A. Squire, and S. C. Moore (1982), Tabular icebergs in ocean waves, *Nature*, *297*, 669–671.
- Lazzara, M. A., K. C. Jezek, T. A. Scambos, D. R. MacAyeal, and C. J. van der Veen (1999), On the calving of icebergs from the Ross Ice Shelf, *Polar Geogr.*, *23*, 201–212.
- Long, D. G., J. Ballantyne, and C. Bertoia (2002), Is the number of Antarctic icebergs really increasing?, *Eos Trans. AGU*, *83*, 472–474.
- Longuet-Higgins, M. S. (1950), A theory of the origin of microseism, *Philos. Trans. R. Soc. London, Ser. A*, *243*, 1–35.
- Melville, W. K. (1996), The role of surface-wave breaking in air-sea interaction, *Annu. Rev. Fluid. Mech.*, *28*, 279–321.
- Müller, C., V. Schlindwein, A. Eckstaller, and H. Miller (2005), Singing icebergs, *Science*, *310*, 1299.
- Munk, W. H., G. R. Miller, F. E. Snodgrass, and N. F. Barber (1963), Directional recording of swell from distant storms, *Philos. Trans. R. Soc. London, Ser. A*, *255*, 505–584.
- Romero, M. C. R. (2004), Analysis of tremor activity at Mt. Erebus Volcano, Antarctica, MS thesis, 159 pp., N.M. Inst. of Min. and Technol., Socorro.
- Snodgrass, F. E., G. W. Groves, K. F. Hasselmann, G. R. Miller, W. H. Munk, and W. H. Powers (1966), Propagation of ocean swell across the Pacific, *Philos. Trans. R. Soc. London, Ser. A*, *259*, 431–497.
- Talandier, J., O. Hyvernaud, E. A. Okal, and P.-F. Piserchia (2002), Long-range detection of hydroacoustic signals from large icebergs in the Ross Sea, Antarctica, *Earth Planet. Sci. Lett.*, *203*, 519–534.
- Whittaker, L. M., and L. H. Horn (1984), Northern hemisphere extratropical cyclone activity for four mid-season months, *J. Climatol.*, *4*, 297–310.
- Zwally, H. J., M. A. Beckley, A. C. Brenner, and M. B. Giovinetto (2002), Motion of major ice-shelf fronts in Antarctica from slant-range analysis of radar altimeter data, 1978–98, *Ann. Glaciol.*, *34*, 255–262.
- R. C. Aster, Geophysical Research Center and Department of Earth and Environmental Science, New Mexico Institute of Mining and Technology, Socorro, NM 87801, USA.
- J. N. Bassis and H. A. Fricker, Institute for Geophysics and Planetary Physics, Scripps Institution of Oceanography, University of California, San Diego, La Jolla, CA 92093, USA.
- K. M. Brunt, L. M. Cathles, Y.-J. Kim, D. R. MacAyeal, and M. H. Okal, Department of the Geophysical Sciences, University of Chicago, Chicago, IL 60637, USA. (drm7@midway.uchicago.edu)
- R. Drucker and S. Martin, School of Oceanography, University of Washington, Seattle, WA 98195, USA.
- E. A. Okal, Department of Geological Sciences, Northwestern University, Evanston, IL 60208, USA.
- M. P. Sponsler, Stormsurf, Half Moon Bay, CA 94019, USA.
- J. E. Thom, Antarctic Meteorological Research Centre, University of Wisconsin, Madison, WI 54025, USA.
- O. V. Sergienko, Hydrospheric and Biospheric Sciences Laboratory, NASA Goddard Space Flight Center, Greenbelt, MD 20771, USA.